Study of a Mo–Au TES deposited directly on a freestanding membrane

J.E. Olsen[a,*], E.C. Kirk[a], Ph. Lerch[a], M.E. Huber[b], K. Arzner[a],
W. Hajdas[a], A. Zehnder[a], H.R. Ott[c]

[a] Paul Scherrer Institute, CH-5232 Villigen, Switzerland
[b] University of Colorado, Denver, CO 80217, USA
[c] ETH-Hönggerberg, CH-8093 Zürich, Switzerland

Abstract

Transition edge sensor devices made with Mo–Au proximity bilayer thermometers have been fabricated. The bilayers were DC-sputter deposited directly on 250 nm thick pre-etched Si_3N_4 membranes. Mo was deposited at 700°C, whereas Au was deposited at room temperature in the same pumpdown in order to allow for a good proximity effect. The superconducting transition temperature of devices with 43 nm Mo and 200 nm Au was around 190 mK. The transition width of bilayers deposited on membranes was substantially larger than those measured on samples deposited on the bulk substrate in the same fabrication run (≈ 2 mK). We consider this difference to be the result of a large temperature gradient across the membrane during the deposition process. Devices were tested with a single stage SQUID array kept at 2.2 K. The resolution of a device that has a transition width of 30 mK is 30 eV at 6 keV. A detailed study shows that the detector noise roughly scales with αI_0, confirming the importance of thermal fluctuation noise in the thermometer.
© 2003 Published by Elsevier B.V.

PACS: 85.25.Oj

1. Introduction

TES microcalorimeters [1] require an absorber in good thermal contact with a sensitive thermometer which in turn has a weak contact with a thermal bath. The thermometer is a superconducting film deposited on a thin membrane of Si_3N_4. The membrane structure is usually obtained by etching of the underlying Si from the original Si_3N_4/Si substrate. One approach is to first deposit the thermometer on a Si_3N_4/Si substrate and then to etch away Si. This route imposes

severe measures to prevent the thermometer from being etched. Future designs will include several pixels and reduced pitch. Protection may become more difficult to realize. We explore the opposite route and fabricate membranes first and follow with the device.

2. Fabrication

First, a Si wafer is coated on both sides with 250 nm thick amorphous Si_3N_4. We define square windows and cleaving grooves into one layer of Si_3N_4 and etch through the Si using a standard KOH solution. This step yields single 12×12 mm^2

substrates with freestanding membranes. A 100 nm thick layer of Nb is DC-sputtered in order to form the electrical contacts. They are shaped using one lithographical step followed by wet etching (H_2O:HNO_3:HF 6:6:1).

Mo and Au compose the proximity bilayer and are DC-sputtered in one single pumpdown. The 43 nm Mo layer is deposited at 700°C. The substrate is allowed to reach room temperature (4 h) and cleaned for 3 min with a fast atom beam (FAB). The deposition of the 200 nm thick Au layer on the cleaned interface begins ~ 15 s later. A photolithographical step followed by wet etching is used to shape 150×400 μm^2 thermometers ($C_v = 0.3$ pJ/K). The Au etch used (KI:I_2:H_2O 4:1:40) is found to etch Mo as well when in the presence of Au. We observe that the etching rate for Mo is even higher than for Au, this produces a slight underetch at the edges of the device and is used to favor normal metal boundary conditions [2]. On each chip there is one series of samples on suspended Si_3N_4 membranes and one on Si_3N_4/Si.

3. Characterization

In Fig. 1 we present the variation of resistance with temperature for two bilayers. The device deposited on Si_3N_4/Si has a much sharper transition than its companion made on Si_3N_4. This difference cannot be explained by self-heating, (max 0.1 pW) since the tail of the transitions occur almost at the same temperature. Again, both bilayers were processed together on the same wafer. We suppose that the severe difference in transition width is due to a temperature gradient created across the membrane during the sputter deposition. This gradient is likely to create mechanical stress which may induce a non-homogeneous film growth. We thermally cycled the sample 15 times during a period of several month and did not notice any changes, however.

4. Experiment

The detector and a 1.4 mΩ thin film Au shunt are mounted in a custom made dilution refrig-
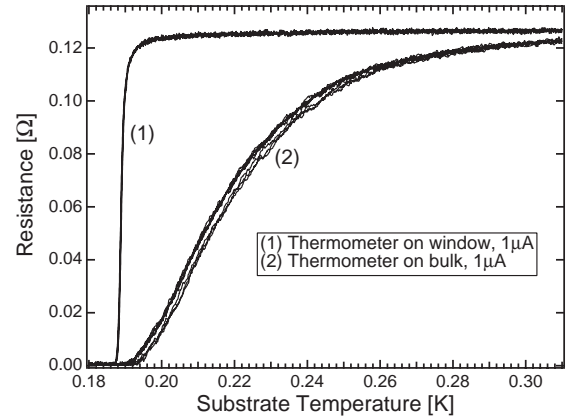

Fig. 1. Several superposed resistance vs. temperature sweeps of two Mo/Au bilayers.

erator reaching 50 mK. The TES is connected in series with the input coil of a single stage DC-SQUID array using a 10 cm long twisted pair of NbTi/Cu. Al wire bonds connect to the device whereas Nb wire bonds [3] connect to the input coil. A bulk Nb can placed at 2.2 K shields the SQUID. The feedback line includes a 2 kΩ resistor thermally anchored at 2.2 K and connected to a feedback unit. An uncollimated source of 6 keV photons illuminates the device.

We studied the performance of our TES operated in negative electrothermal feed back mode. The equilibrium TES resistance R_0 was varied and data sets of 2000 pulses containing 4000 points each were recorded at a sampling rate of 2.5×10^6 s^{-1}. A typical 6 keV pulse is shown in the inset of Fig. 2. The height of each pulse is estimated using an optimal filter template constructed for each data set individually, as described in Ref. [4]. In Fig. 2 (top) we show the best 6 keV pulse height spectrum with a resolution of $\Delta E = 30$ eV (FWHM). This kind of performance is achieved for $7 < R_0 < 30$ mΩ. The dependence of ΔE on R_0 is shown in the lower part of Fig. 2. The performance loss at high R_0 values is due to the pulse amplitude reduction that follows the reduction of $\alpha = $ d log $R/$d log T. At very low R_0 values, however, the detector is less stable as revealed by the enhanced scattering of the data together with the general increase of ΔE. The stability of the SQUID needs also to be taken into account.
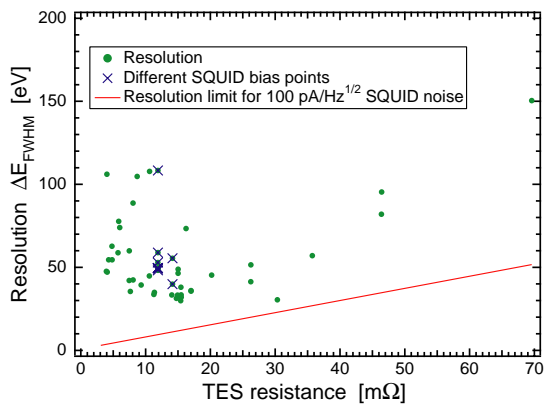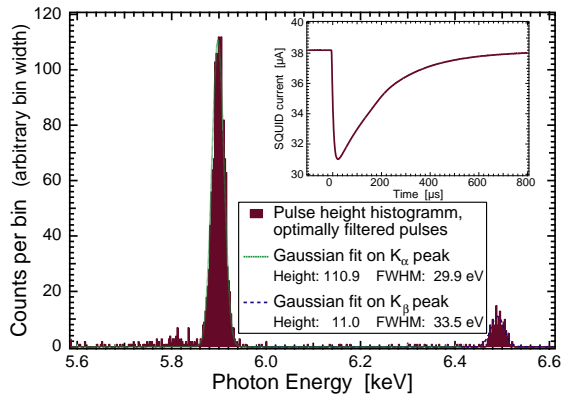
Fig. 2. Top: Best 6 keV pulse height spectrum measured at $R_0 = 15$ mΩ. Bottom: Resolution vs. TES equilibrium resistance R_0.

Fig. 3. Top: spectral densities of signal and noise; bottom, signal noise vs. αI_{eq}.

Minute variations of the bias point of the SQUID affect detector performances. The current noise of the SQUID is measured ≈ 100 pA/$\sqrt{\text{Hz}}$. The corresponding resolution limit has been estimated assuming an ideal signal processing with an infinite bandwidth [5] and is shown as a straight line on the graph.

We performed a detailed noise study. For each data set, we calculated the power spectral density (PSD) of the signal displayed i on the Fig. 3 top. Using an averaged pulse form we estimated the PSD of an ideal signal, ii. The difference of these PSD represents the signal noise, iii. Surprisingly, no clear correlation between the noise level and the energy resolution could be extracted. The main noise contributions [6] are also displayed.

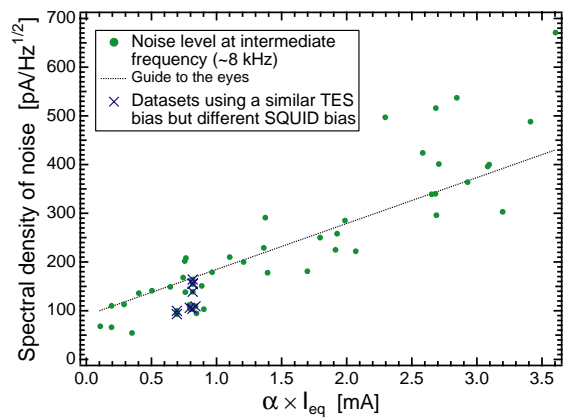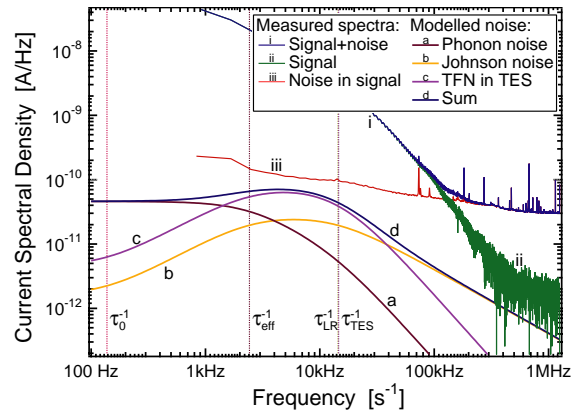The thermal fluctuation noise (TFN) in the device, which is expected to scale with αI_{eq},

dominates at intermediate frequencies. This fact is confirmed in Fig. 3 (bottom) which shows the noise level at 8 kHz as a function of αI_{eq}.

5. Conclusion

The advantage of a fabrication route using membranes to begin with is compensated by the presence of a thermal gradient during the deposition of Mo. The superconducting transition width of Mo/Au bilayers deposited on hot membranes are much wider than for bilayers deposited on hot but bulk substrates of the same material. The wider transition width limits the TESs performances. Best energy resolution (30 eV–6 keV) is achieved if R_0 ranges between 7 and 30 mΩ, $R_n = 120$ mΩ. The scattering observed in the resolution

data at low R_0 cannot be explained by excess noise only.

Acknowledgements

References

[1] W.M.B. Tiest, et al., AIP Conf. Proc. 605 (2002) 199.
[2] K.D. Irwin, et al., Nucl. Instr. and Meth. A 444 (2000) 184.
[3] W. Jaszczuk, et al., Meas. Sci. Technol. 2 (1991) 1121.
[4] A.E. Szymkowiak, et al., J. Low Temp. Phys. 93 (1993) 281.
[5] S.H. Moseley, et al., J. Appl. Phys. 56 (1984) 1257.
[6] H.F.C. Hoevers, et al., Appl. Phys. Lett. 77 (2000) 4422.